Nanowell-Based Immunoassays for Measuring Single-Cell Secretion: Characterization of Transport and Surface Binding

Alexis J. Torres[†], Abby S. Hill[‡] and J. Christopher Love*[,†,§]

[†]Department of Chemical Engineering, Massachusetts Institute of Technology, Cambridge, MA 02139.

[‡]Department of Biological Engineering, Massachusetts Institute of Technology, Cambridge, MA 02139.

[§]Koch Institute for Integrative Cancer Research, Massachusetts Institute of Technology, Cambridge, MA 02139.

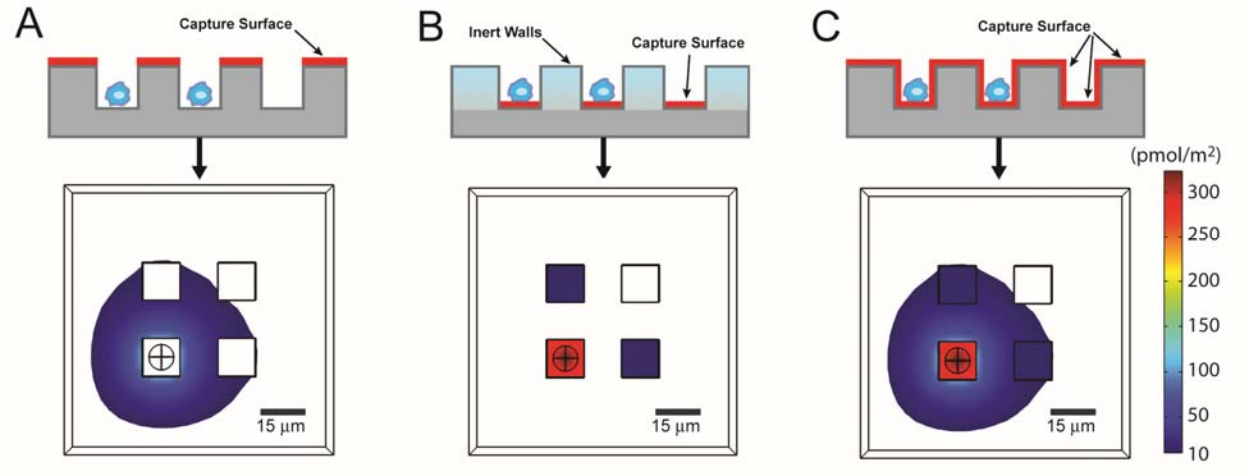

Figure S1: Comparison of theoretical surface capture of secreted antibody (from single cells) in the configuration developed here and previously reported configurations. A) Surface binding of analyte on a device where only the top surface has been modified with capture antibody [10]. B) Configuration in which binding occurs only at the bottom surface of the wells; the sidewalls consist of an inert polyethylene glycol hydrogel to prevent absorption to the walls [5]. C) Surface binding of analyte on a device where the entire surface has been uniformly modified with capture antibody. The capture efficiency of secreted analyte increases by more than an order of magnitude in configurations (B) and (C). Simulations were performed using a capture ligand of moderate affinity (K_d = 10 nM) and a secretion rate of 1000 molecules/s.

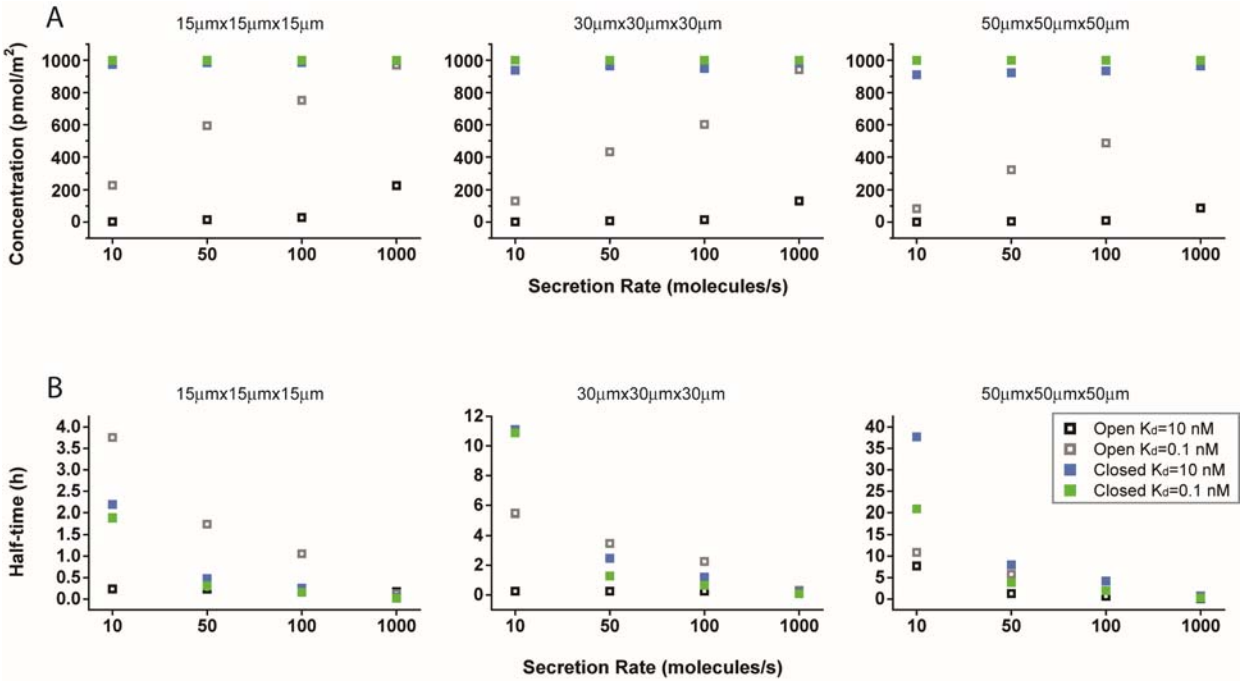

Figure S2: Theoretical analysis of analyte surface binding on the capture surface in an open system (in-well capture) or closed system (microengraving) configuration. A) Maximal concentration of surface bound protein at steady-state. B) Half-time to reach steady-state. Nanowells of different dimensions were used in these simulations. The labels indicate the dimensions of the wells and the legend specifies the dissociation binding constant and configuration.

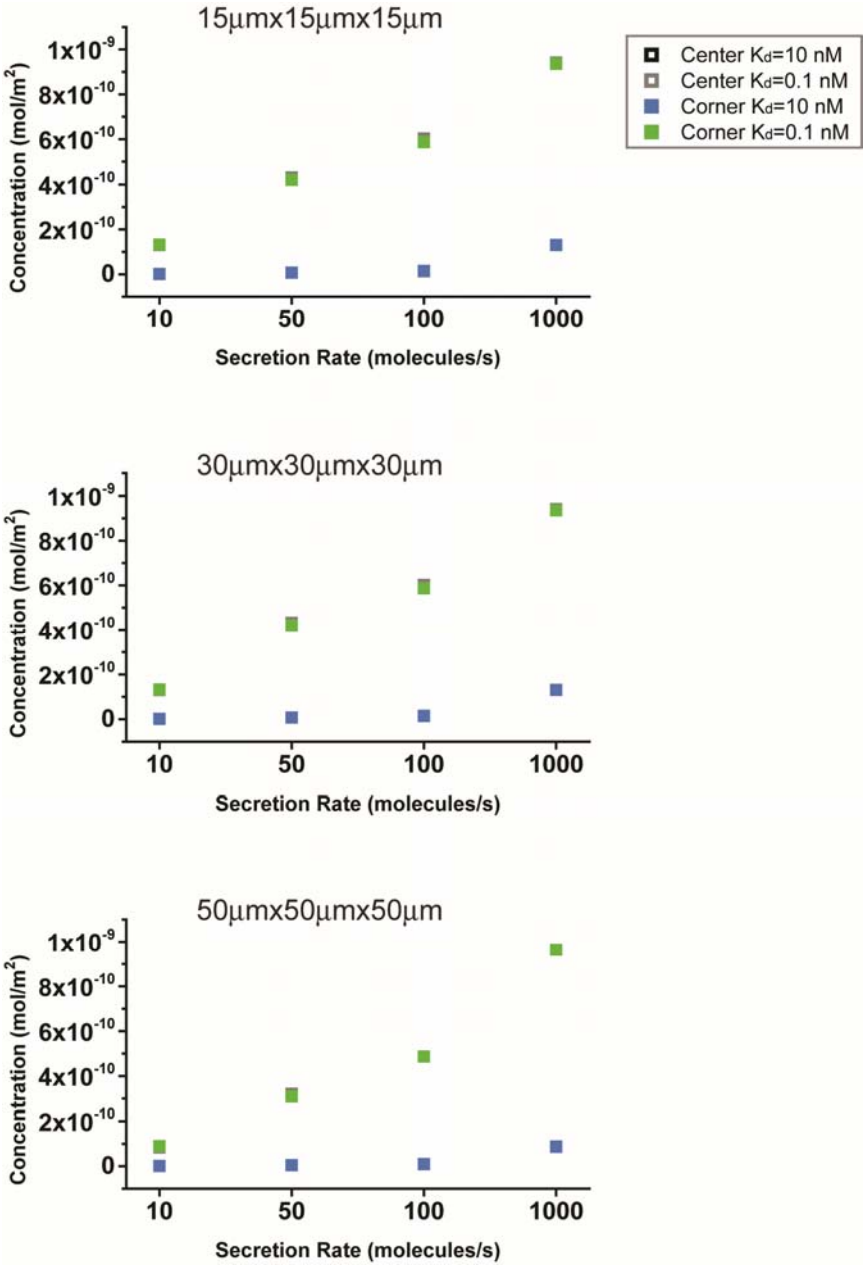

Figure S3: Effects of deviation from centralized positioning of the cell in the wells for the in-well capture configuration. Plots of the maximal binding at equilibrium calculated when a cell was positioned in the center of the basal surface of the well or in the corner of the well.

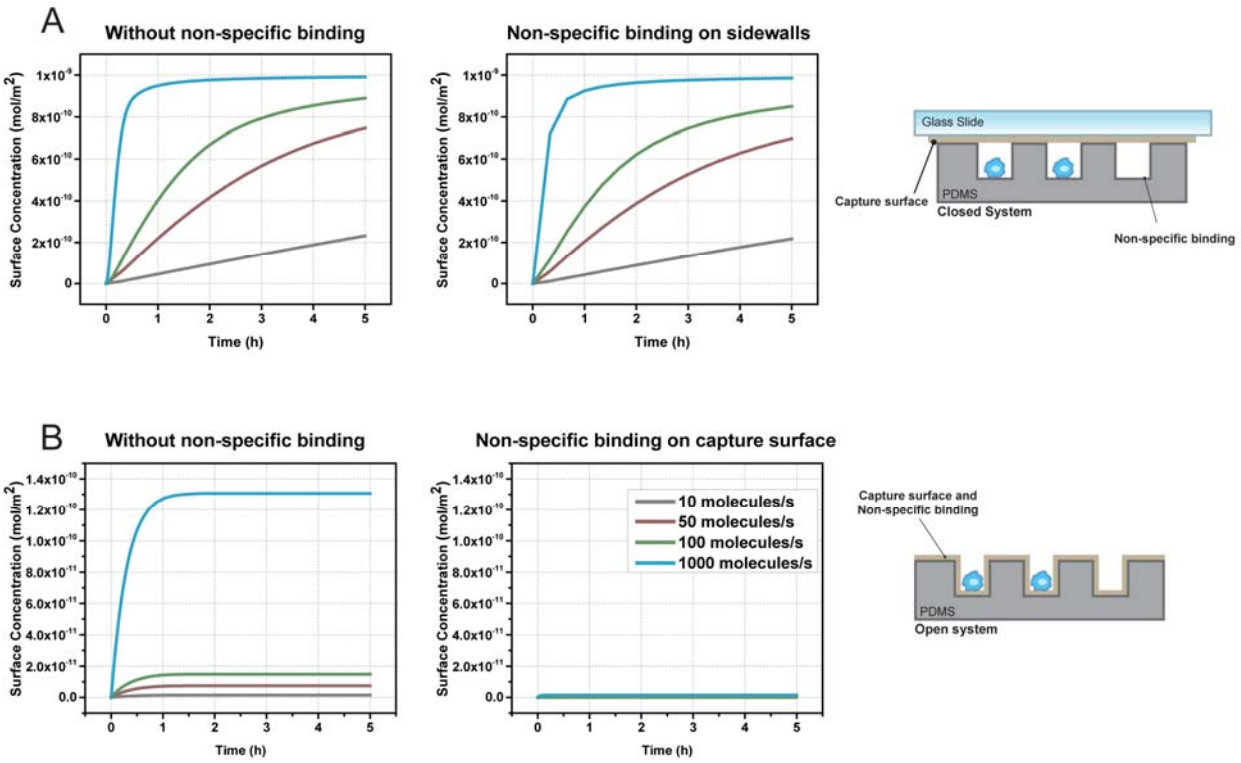

Figure S4: Effects of non-specific binding. A) Plots of the calculated surface concentration of captured analytes on a glass slide with microengraving when the surface of the nanowells is impervious to non-specific binding of analyte (left plot) compared with the case in which non-specific binding occurs (center). Schematic illustrates the configuration of the system used (right). B) Plots of the calculated surface concentration of analytes captured specifically on the surfaces of the nanowells in the open-well configuration when the surface of the nanowells is impervious to non-specific binding of analyte (left plot) compared with the case in which analytes are retained only through non-specific binding (center). Schematic illustrates the configuration of the system used (right). Non-specific binding was assumed to be in the μM range (K_d=1μM, k_{on}=1x10^4 1/(M s), k_{off}=1x10^{-2} s^{-1}), and specific binding was based on K_d=10 nM.